Rev.Adv.Mater.Sci. 4 (2003) 60-64

OPTICAL AND STRUCTURAL PROPERTIES OF Li, Zn, Ag and Au NANOCLUSTERS EMBEDDED IN MgO

M.A. van Huis [1], A. van Veen[1], H. Schut[1], S.W.H. Eijt[1], B.J. Kooi[2], J.Th.M. De Hosson[2] and T. Hibma[2]

[1]Interfaculty Reactor Institute, Delft University of Technology, Mekelweg 15, NL 2629 JB Delft, The Netherlands
[2]Materials Science Center, University of Groningen, Nijenborg 4, NL 9747 AG Groningen, The Netherlands

Received: December 05, 2002

Abstract. Lithium, zinc, silver and gold nanoclusters (NCs) embedded in MgO were created by means of ion implantation of Li, Zn, Ag and Au ions into single crystals of MgO (100) and subsequent thermal annealing. Optical and structural properties of the NCs were investigated using optical absorption spectroscopy (OAS), high-resolution X-ray diffraction (XRD) and cross-sectional transmission electron microscopy (XTEM). The mean nanocluster size is estimated from the broadening of the Mie plasmon optical absorption bands using the Doyle formula. These results are compared with the NC size as obtained from XRD (using the Scherrer formula) and from direct XTEM observations. The three methods are found to be in reasonable agreement with a mean size of 4.0 and 10 nm found for the Au and Ag clusters, respectively. Using TEM observations, the relative interface energies of MgO//Au and MgO//Ag interfaces are also determined. In the case of MgO//Au, they are found not to be in agreement with theoretical predictions in the literature.

1. INTRODUCTION

Metal and semiconductor nanoclusters embedded in transparent matrices exhibit linear and non-linear optical properties that are of interest to the field of opto-electronics [1,2]. A feasible way of producing these clusters is by means of ion implantation and subsequent annealing [3,4]. The cluster size can be estimated from the broadening of the optical absorption peak that is present as a result of Mie plasmon resonance [4]. Here, the Doyle theory [5] is used to estimate the nanocluster size during the annealing procedure. Alternatively, the size can be estimated from the broadening of the XRD diffraction peaks using the Scherrer formula [6]. In this work, we compare the nanocluster size as obtained from the three methods mentioned above. Using the Wulff plot [7, 8] applied to HRTEM results, we also discuss the interface energies of MgO//Au and MgO//Ag interfaces, and compare them with theoretical results from the literature.

2. EXPERIMENTAL

In order to create a subsurface layer of nanoclusters, epi-polished MgO(100) single crystals of size 10x10x1 mm^3 were implanted at room temperature with $1.0 \cdot 10^{16}$ Au, Ag or Li ions cm^{-2} at an energy of 1.0 MeV, 600 keV and 30 keV, respectively. The 140 keV Zn ions were implanted at room temperature to a higher fluence of $1.0 \cdot 10^{17}$ ions cm^{-2}. After ion implantation, the MgO:Li and MgO:Zn samples were annealed for 1 hr in ambient air at a temperature of 1100K and 1150K, respectively. The MgO:Ag and MgO:Au samples were annealed at 1500K for a period of 22 hrs. An overview of the sample treatment data is given in Table 1. Optical absorption spectroscopy (OAS) was performed using a Perking Elmer Lambda 40 spectrometer. Structural properties were studied using high-resolution X-ray diffraction (XRD) and cross-sectional transmission electron microscopy (XTEM). The XRD measurements were performed using a Philips X'Pert materials research diffractometer system; a ceramic X-ray tube provided Cu $K\alpha$ radiation. The TEM was performed

Corresponding author: M.A. van Huis, e-mail: vanhuis@iri.tudelft.nl

Table 1. Sample treatment and structural properties of the Li, Zn, Ag and Au NCs (see also Ref. [12]).

	Li	Zn	Ag	Au
Sample treatment				
implantation dose (cm^{-2})	10^{16}	10^{17}	10^{16}	10^{16}
energy (keV)	30	140	600	1000
annealing temperature (K)	1100	1150	1473	1473
time (hrs)	0.5	0.5	22	22
Material properties				
Lattice parameter (Å)	4.40 (fcc)	–	4.085(fcc)	4.078(fcc)
(MgO: 4.212 Å, fcc)	3.51 (bcc)			
Fermi velocity v_F ($m \cdot s^{-1}$) [10]	$1.29 \cdot 10^6$	$1.82 \cdot 10^6$	$1.38 \cdot 10^6$	$1.38 \cdot 10^6$
Position centroid abs. peak				
predicted λ_{max} (nm), Eq. (2)	549	331	449	537
observed λ_{max} (nm), Fig. 1	535	288	538	565
Cluster size				
· using Doyle (nm), Eq. (1)	1.8	1.9	5.1	4.3
· using XRD (nm), Eq. (3)	– [a]	–	9.8	4.0
(Scherrer constant K_w)			(0.8863)	(0.8290)
· XTEM mean size (nm)	– [a]	–	11	4.6

[a] not observable.

using a JEOL 4000 EX/II operating at 400 kV (point-to-point resolution 0.17 nm). The specimen preparation is discussed elsewhere [9].

3. RESULTS AND DISCUSSION

3.1. Optical properties

The results of the optical absorption measurements are displayed in Fig. 1 for MgO containing Li, Zn, Ag and Au NCs. The Mie plasmon resonance optical absorption bands are additionally broadened due to plasmon quantum confinement (see below), NC size dispersion and interface effects with the MgO. In the Doyle theory, the mean free path of the electrons constituting the plasmon is limited by the size of the nanocluster. Neglecting size dispersion and interface effects, the cluster size can be estimated using [5]

$$D = 2\frac{\upsilon_F}{\Delta\omega_{1/2}} = 2\frac{\upsilon_F}{2\pi c}\frac{\lambda_{max}^2}{\Delta\lambda_{1/2}}. \qquad (1)$$

Here D is the diameter of the precipitate (m), υ_F the Fermi velocity ($1.29 \cdot 10^6$ m/s for lithium, $1.82 \cdot 10^6$ m/s for Zn and $1.39 \cdot 10^6$ m/s for both gold and silver [10]), $\Delta\omega_{1/2}$ the FWHM of the peak when plotted as a function of the angular frequency ω (rad/s), c the speed of light (m/s), λ_{max} the position of the centroid of the peak and $\Delta\lambda_{1/2}$ the FWHM of the peak when plotted as a function of wavelength (m). The FWHM of the absorption peak in Fig. 1 and the parameters

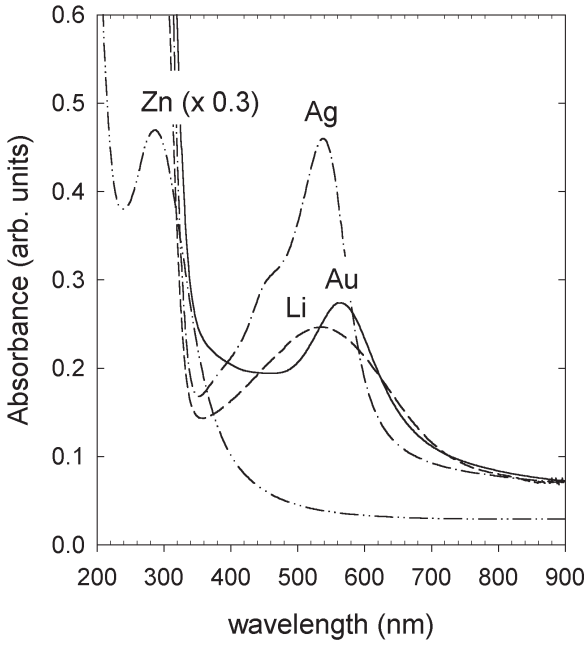

Fig. 1. Optical absorption spectra showing the Mie plasmon absorption band of MgO containing Li, Zn, Ag and Au NCs.

mentioned above were substituted in Eq. (1), yielding cluster diameters of 1.8, 1.9, 5.1 and 4.3 nm for the Li, Zn, Ag and Au clusters, respectively. In the case of the Zn clusters, a systematic error is introduced because the position of the peak coincides with the F-centers of the MgO host matrix. The position of the centroid (λ_{max}) can be estimated using the following relationship [4]:

$$\varepsilon_1(\omega_p) + 2n_0^2 = 0. \qquad (2)$$

Here ε_1 is the real part of the dielectric constant of the metal and n_0 the refractive index of MgO, which equals 1.74. Considering the dielectric constants of Zn [11], this condition is satisfied when $\lambda=2\pi c/\omega_p$ equals 330 nm, in reasonable agreement with the λ_{max} of the Zn plasmon resonance peak in Fig. 1. The optical properties are summarised in Table 1, which includes also the predicted and observed positions of the centroids for Li, Zn, Ag and Au.

3.2. Structural properties

High-resolution XRD measurements were carried out on the MgO(002), (113), (004) and (024) diffraction peaks for MgO:Ag and MgO:Au. Silver and gold atoms have many electrons so that the detection of the XRD peaks is feasible despite the low total amount of implanted ions. The crystal structure of MgO, Au and Ag is fcc and the Au and Ag NCs are in a cube-on-cube orientation relationship with MgO. The relevant lattice parameters are listed in Table 1. Because the lattice parameters of Au and Ag are close to that of MgO, Au(113) and Ag(113) satellite peaks are observed near the intense MgO(113) peaks [12]. The cluster size was estimated from the width of the Au and Ag(113) diffraction peaks using the Scherrer formula [6]

$$p = K_w \frac{\lambda_0}{\Delta\theta \cos\theta} = K_w \frac{2}{\Delta k \sqrt{h^2 + k^2 + l^2}}. \qquad (3)$$

Here p is the precipitate size, defined as the cube root of the precipitate volume. Furthermore, λ_0 is the wavelength (1.540560 Å), θ the position of the (hkl) diffraction peak, $\Delta\theta$ the FWHM of the same diffraction peak and Δk the FWHM of the peak in reciprocal space in m^{-1}. The half-width Scherrer constant K_w depends on the shape of the nanocluster and on the *(hkl)* index of the diffraction peak [6]. The results of the Scherrer analysis [12] are shown in Table 1. The XTEM results on these samples are discussed in Ref. [12] and the results are also shown in Table 1. Comparing the NC cluster sizes as obtained from optical absorption, XRD and XTEM, it can be concluded that the cluster sizes are in reasonable agreement, although the size of the Ag clusters as deduced using the Doyle formula underestimates the size (as observed by TEM). Possibly the Ag clusters are already too large for application of Doyle-Mie theory.

Figs. 2 and 3 show TEM observations of Au and Ag NCs embedded in MgO. It is clear that in Fig. 2, the Au clusters are spherically shaped, i.e., the {100} and {110} facets are equally large. In Fig. 3 however, the Ag clusters are shaped as truncated octahedrons. These two samples were annealed in ambient air. When the annealing takes place in vacuum or in a reducing environment, the Au clusters adopt a cubical shape [13] while the Ag clusters maintain an octahedral shape after vacuum anneal [14]. Apparently, the interface energy corresponding to a particular facet is dependent on the oxygen pressure in the MgO. If the interface energies are known, the morphology of the clusters can be constructed using the so-called Wulff plot [7, 8]. The length of the vector from the center of the NC to a particular facet is proportional to the interface energy of that facet, as indicated in Fig. 3 for a Ag cluster. The interface energies can be determined from the sur-

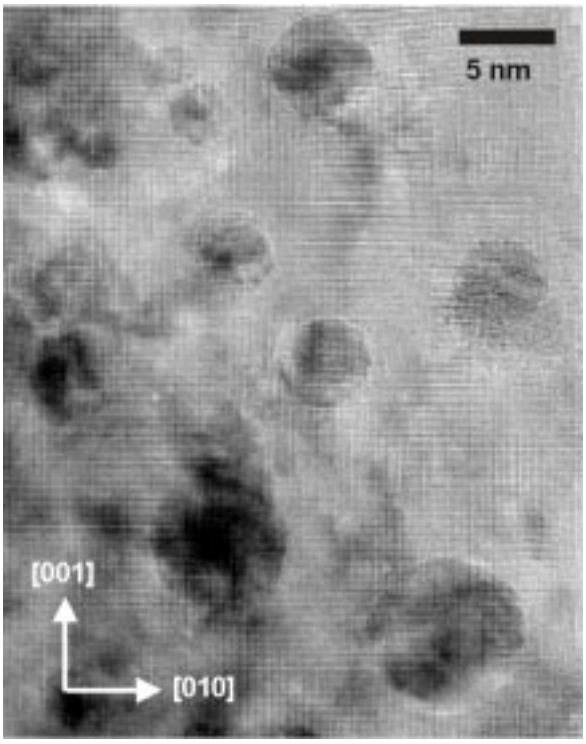

Fig. 2. HR TEM image of a few gold clusters in a cube-on-cube orientation relationship with the embedding MgO matrix. The anneal was performed in ambient air at 1473K.

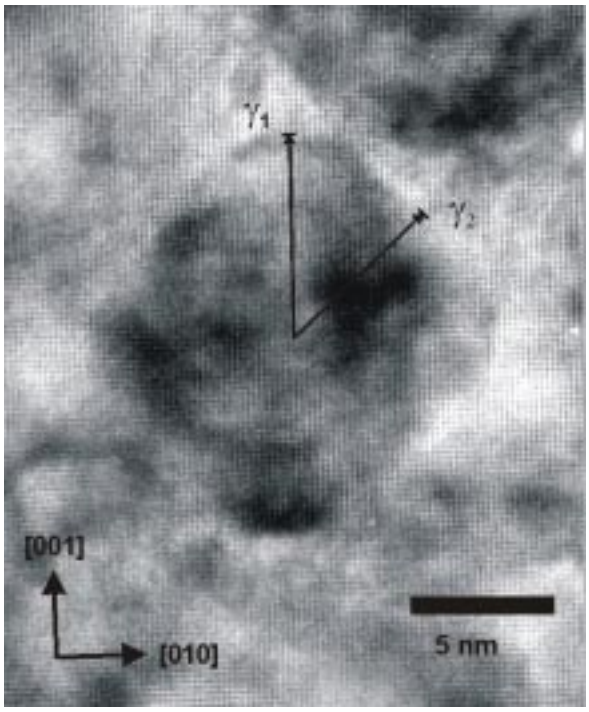

Fig. 3. HR TEM image of silver clusters in a cube-on-cube orientation relationship with the embedding MgO matrix. The anneal was performed in ambient air at 1473K.

Table 2. Surface energies and works of adhesion obtained from the literature; calculated interface energies for the {001} and {011} facets of MgO//Au and MgO//Ag using Eq. (4).

Surface energies Surface	γ (Jm^{-2})	Ref.
MgO{001}	1.20	[15]
MgO{011}	2.87	[15]
Au{001}	1.50	[16]
Au{011}	1.56	[16]
Ag{001}	1.31	[16]

Interface energies Interface	W_{ad} (Jm^{-2})	using Eq. (4) γ_{int} (Jm^{-2})	Ref. for W_{ad}
$MgO_{\{001\}}//Au_{\{001\}}$	1.28	1.4	[17]
$MgO_{\{011\}}//Au_{\{011\}}$	0.89	3.5	[17]
$MgO_{\{001\}}//Ag_{\{001\}}$	1.44	1.1	[17]
$MgO_{\{111\}}//Ag_{\{111\}}$	–	–	

face energies of the MgO, the metal, and the work of adhesion W_{ad} as

$$\gamma_{interface} = \gamma_{MgO} + \gamma_{metal} - W_{ad} . \quad (4)$$

Data for γ_{MgO}, γ_{metal} and W_{ad} were retrieved from the literature and are given in Table 2. From the interface energies, interface energy ratios such as $\gamma_{\{011\}}/\gamma_{\{001\}}$ can be calculated and compared to the ratio observed experimentally in TEM images. In the case of the Ag cluster in Fig. 3, the shape is so close to octahedral because of the large {111} interfaces [8]. Therefore, the vector γ_2 displayed in Fig. 3 does not point to a {011} interface, but to the intersection of the {1 1 1} and {-1 1 1} interfaces. In that case, $\gamma_{\{111\}} = 1/3\sqrt{6}\,\gamma_2$. The interface energy ratios found are listed in Table 3. Unfortunately, the work of adhesion for the $MgO_{\{111\}}//Ag_{\{111\}}$ interface is not known from literature.

It is clear that the theoretical prediction for MgO//Au does not agree with the experimental observations. This is probably due to the high surface energy of the MgO {011} surface, which in reality might be in a reconstructed configuration [15]. Another point of concern is that the calculated works of adhesion vary widely in the literature, depending on the computational method used [18]. From the experimental observations, the Au NCs seem to be more affected by the oxygen pressure than the Ag NCs.

4. CONCLUSIONS

A reasonable first-order estimate of the NC cluster size can be found using the Doyle formula for the broadening of the Mie plasmon absorption peak. Using the Scherrer formula applied to XRD peaks yields values for the mean cluster size that are very close to the result of XTEM observations. Relative interface energies for MgO//Au and MgO//Ag interfaces were determined using the Wulff plot applied to TEM images of Au and Ag clusters. It can be concluded that the theoretical predictions found in the literature do not agree well with the experimental observations for MgO//Au.

REFERENCES

[1] P. Chakraborty // *J. Mater. Sci.* **33** (1998) 2235.
[2] K. Fukumi, A. Chayahara, K. Kodano, T. Sakaguchi, Y. Horino, M. Miya, K. Jujii,

Table 3. Ratio of interface energies, theoretical and experimental values.

Interface	*method*	*anneal*	*ratio*	*Ref.*
		γ{011}/γ{001}		
MgO//Au	theor.		2.5	Table 2
	exp.	air	1.0	this work, Fig. 2
	exp.	vacuum	1.3	[13]
		γ{111}/γ{001}		
MgO//Ag	theor.		not known	–
	exp.	air	0.69	this work, Fig. 3
	exp.	vacuum	0.73	[14]

J. Hayakawa and M. Satou // *J. Appl. Phys.* **75** (1994) 3075.

[3] C.W. White, J.D. Budai, S.P. Withrow, J.G. Zhu, E. Sonder, R.A. Zuhr, A. Meldrum, D.M. Hembree Jr., D.O. Henderson and S. Prawer // *Nucl. Instrum. Meth. Phys. Res. B* **141** (1998) 228.

[4] R.L. Zimmerman, D. Ila, E.K. Williams, D.B. Poker, D.K. Hensley, C. Klatt and S. Kalbitzer // *Nucl. Instrum. Meth. Phys. Res. B* **148** (1999) 1064, and references therein.

[5] W.T. Doyle // *Phys. Rev.* **111** (1958) 1067.

[6] J.I. Langford and A.J.C. Wilson // *J. Appl. Cryst.* **11** (1978) 102.

[7] H. Lüth, *Surfaces and Interfaces of Solid Materials* (Springer-Verlag, Berlin, 1995).

[8] M. Backhaus-Ricoult // *Acta Mater.* **49** (2001) 1747.

[9] B.J. Kooi, A. van Veen, J.Th.M. de Hosson, H. Schut, A.V. Fedorov and F. Labohm // *Appl. Phys. Lett.* **76** (2000) 1110.

[10] C. Kittel, *Introduction to Solid State Physics* (John Wiley&Sons, New York, 1986).

[11] G.W. Rubloff // *Phys. Rev. B* **3** (1971) 285.

[12] M.A. van Huis, A.V. Fedorov, A. van Veen, C.V. Falub, S.W.H. Eijt, B.J. Kooi, J.Th.M. De Hosson, T. Hibma and R.L. Zimmerman // *Nucl. Instrum. Meth. Phys. Res. B* **191** (2002) 442.

[13] E.M. Bryant, A. Ueda, R.R. Mu, M.H. Wu, A. Meldrum and D.O. Henderson // *Mater. Res. Soc. Symp. Proc.* **635** (2001) C1.5.

[14] G. Abouchacra and J. Serughetti // *Nucl. Instrum. Meth. Phys. Res. B* **14** (1986) 282.

[15] M.B. Taylor, C.E. Sims, G.D. Barrera, N.L. Allan and W.C. Mackrodt // *Phys. Rev. B* **59** (1999) 6742.

[16] H. Cox, X. Liu and J.N. Murrell // *Molecular Physics* **93** (1998) 921.

[17] D.M. Duffy, J.H. Harding and A.M. Stoneham // *Phil. Mag. A* **67** (1993) 865.

[18] J. Purton, D.M. Bird, S.C. Parker and D.W. Bullett // *J. Chem. Phys.* **110** (1999) 8090.